COMPOSITION OF ANOMALOUS COSMIC RAYS AND IMPLICATIONS FOR THE HELIOSPHERE

A. C. CUMMINGS and E. C. STONE
California Institute of Technology, Pasadena, CA 91125

Abstract. We use energy spectra of anomalous cosmic rays (ACRs) measured with the Cosmic Ray instrument on the Voyager 1 and 2 spacecraft during the period 1994/157-313 to determine several parameters of interest to heliospheric studies. We estimate that the strength of the solar wind termination shock is 2.42 (-0.08, +0.04). We determine the composition of ACRs by estimating their differential energy spectra at the shock and find the following abundance ratios: H/He = 5.6 (-0.5, +0.6), C/He = 0.00048 $\pm$ 0.00011, N/He = 0.011 $\pm$ 0.001, O/He = 0.075 $\pm$ 0.006, and Ne/He = 0.0050 $\pm$ 0.0004. We correlate our observations with those of pickup ions to deduce that the long-term ionization rate of neutral nitrogen at 1 AU is $\sim 8.3 \times 10^{-7}$ s^{-1} and that the charge-exchange cross section for neutral N and solar wind protons is $\sim 1.0 \times 10^{-15}$ cm^2 at 1.1 keV. We estimate that the neutral C/He ratio in the outer heliosphere is $1.8(-0.7, +0.9) \times 10^{-5}$. We also find that heavy ions are preferentially injected into the acceleration process at the termination shock.

Key words: abundances, anomalous cosmic rays, *Voyager*, interstellar medium, heliosphere, solar wind termination shock

1. Introduction

Anomalous cosmic rays (ACRs) are energetic particles which are thought to be accelerated pickup ions. The main acceleration is thought to take place at the solar wind termination shock (Pesses et al., 1981). The source of the pickup ions that become ACRs is believed to be neutral gas from the interstellar medium (Fisk et al., 1974). The ACR component currently consists of seven elements: H, He, C, N, O, Ne, and Ar (Garcia-Munoz et al., 1973; McDonald et al., 1974; Hovestadt et al., 1973; Cummings and Stone, 1988, 1990; Christian et al., 1988, 1995; McDonald et al., 1995). Previous studies of their composition have led to estimates of the abundances of neutral gas in the interstellar medium (Cummings and Stone, 1987, 1990). However, those studies were made before the pickup ion observations became available and the fractionation in the acceleration and propagation processes could only be roughly estimated.

In this study we adopt a new approach that makes use of the pickup ion observations and the ACR observations to gain information on the injection of the pickup ions into the acceleration process at the termination shock. This approach has only become viable as solar modulation has lessened to such an extent that the observed ACR energy spectra are less modulated than at any time in the past. This decreased modulation results in ACR spectra which show signs of a power-law dependence at low energies, which makes possible estimates of the ACR spectra at the shock.

The ACR shock spectra are estimated for H, He, C, N, O, and Ne. Ar, which was included in previous studies, is observable only at energies above the roll-off energy of the shock spectrum. Thus we can gain no information on the low-energy power-law portion of the shock spectrum, which is what is required for this study. Estimates of the neutral densities of H, He, N, O, and Ne in the outer heliosphere (30 - 60 AU) are available from pickup ion studies (Geiss et al., 1994; Geiss and Witte, 1996). We use a model of their ionization and subsequent transport to estimate the fluxes of pickup ions incident on the termination

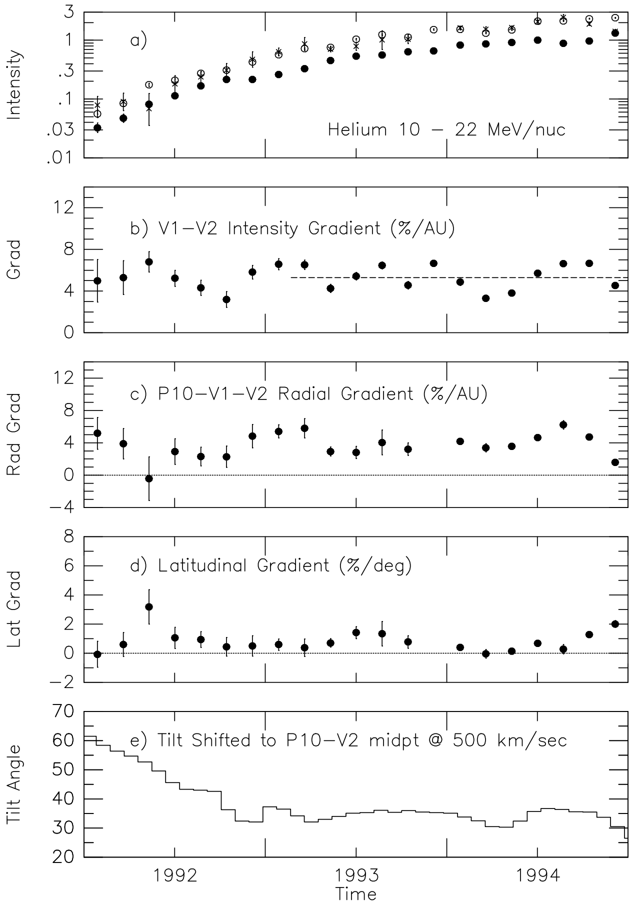

Figure 1. Intensity of helium (52-day averages) measured at P10 (crosses), V2 (solid circles), and V1 (open circles) versus time. b) Intensity gradient between V1 and V2 for He with 9.3 - 22.3 MeV/nuc. The dashed line is the mean for the period indicated. c) Radial gradient of ACR He with $\sim$ 10 - 22 MeV/nuc. d) Latitudinal gradient of ACR He with $\sim$ 10 - 22 MeV/nuc. e) Estimated tilt of the neutral current sheet shifted to the mid-point of V2 and P10. Each tilt observation (Hoeksema, private communication, 1995) covers a single solar rotation or $\sim$ 26 days. We have performed a 3-solar-rotation moving average on the supplied tilt data set before plotting, in order to approximate the average conditions between V2 and P10 which are $\sim$ 17 AU apart.

shock. We use a theory of particle acceleration at the termination shock to estimate the resulting power-law differential energy spectra for these elements. These spectra can be compared with our derived ACR shock spectra to estimate the relative injection efficiencies of pickup ion H^+, He^+, O^+, and Ne^+. We do not have independent information on the charge-exchange cross section of N, so in the case of N we can estimate this quantity and the ionization rate of N at 1 AU by using an estimate of the injection efficiency of pickup ion N^+ based on that of O^+ and Ne^+. Also, by using an estimate of the injection efficiency of C^+, we can estimate the neutral C abundance in the outer heliosphere.

2. ACR Shock Spectra

In order to estimate the ACR shock spectra, we compare our observations made with the Cosmic Ray instrument (Stone et al., 1977) on V1 and V2 during 1994/157-313 with a spherically-symmetric equilibrium model of the propagation of ACRs, including diffusion, convection, and adiabatic deceleration (Fisk, 1971). This period consists of three 52-day periods which were part of a recent study on the distance to the termination shock (Stone et al., 1996). The average latitudinal gradient for ACR He with 10 - 22 MeV/nuc was $\sim$ 0.8%/deg for the period considered in that study, 1993/52 - 1994/365. This latitudinal

Table I
V2 radial shifts from Equation 1

Element	$<T>$ (MeV/nuc)	$<G_{V1V2}>$ (%/AU)	G_{V1V2} (%/AU)	Δr_{V2} (AU)
He	20.1	4.49	5.32	-2.41
	26.0	2.69	3.37	-3.26
	34.8	3.33	3.87	-2.13
	43.9	2.07	2.40	-2.12
O	4.3	3.20	4.75	-6.34
	4.9	3.18	4.66	-6.10
	6.2	3.25	3.91	-2.64
	7.9	2.81	3.51	-3.29
	10.5	2.91	3.52	-2.71

gradient is small enough that we feel justified in using a spherically-symmetric model of propagation to make a first order estimate of the shock spectra, shock location, and other parameters. We will later make a correction to the estimated shock location by accounting for the finite latitudinal gradient.

Figure 1 is reproduced from Figure 2 of Stone et al. (1996) and displays the time history of He with 10 - 22 MeV/nuc, three gradients of these particles, and the tilt of the neutral current sheet. The time period we have chosen for this study, 1994/157-313, comprise the 4th through 6th 52-day periods of 1994 shown in panels a-d of Figure 1. In Figure 1b, intensity gradients between V1 and V2 are shown and it appears that the period 1994/157-313 chosen for this study has a larger than average gradient. The gradient for the period 1993/52 - 1994/365 is seen to wander about a mean value of 5.3%/AU showing no systematic increase or decrease. The non-statistical variations are caused by transient disturbances and ideally we would use a period that was unaffected by such disturbances, as was done in the Stone et al. (1996) study. However, in order to get good statistical precision for the heavier ACR species and to observe ACR H at both V1 and V2, it was necessary to use several of the most recent periods for the analysis.

By examining Figure 1a, we deduce that the transient disturbance during 1994/157-313 is affecting the V2 fluxes, making them lower than they would otherwise be. This atypical gradient can be accounted for in our model fits by moving the V2 spacecraft towards the Sun from its actual position and away from V1. Thus, the intensity we observe at V2 during this transient decrease is representative of the equilibrium intensity at a position some distance sunward of V2.

In order to estimate the effective radial location of V2, we examined the V1/V2 intensity gradients in four He energy intervals and in five O energy intervals for 11 52-day periods (1993/105 - 1994/313) and for the period 1994/157-313. We computed the distance, Δr_{V2}, to move V2 for each energy interval from the equation:

$$\Delta r_{V2} = \frac{< G_{V1V2} > - G_{V1V2}}{< G_{V1V2} >} \left(r_{V1} - r_{V2} \right) \tag{1}$$

where $< G_{V1V2} >$ is the average V1/V2 intensity gradient for the 11 time periods, G_{V1V2} is the observed V1/V2 intensity gradient for the period 1994/157-313, and r_{V1} and r_{V2} are the average radial locations of the V1 and V2 spacecraft, respectively. The average latitudes and radial locations of the spacecraft are 32.5°N and 56.8 AU for V1 and 12.3°S and 43.7

AU for V2. The gradients and radial shifts for V2 calculated from Equation 1 are displayed in Table I. We find that the average V2 correction for the 9 observations is -3.4 $\pm$ 0.5 AU. Thus the effective radial location of V2 for the purposes of the model fits is 40.3 AU.

In the model calculations we fit the ACR H, He, C, N, O, and Ne spectra at V1 and V2. These spectra are obtained by subtracting estimated spectra of galactic cosmic rays from the observed spectra. The estimated GCR spectra for each element were derived from the observed C and O spectra at high energies. For V1, a power-law fit, with the spectral index fixed at 1.0, was made to three C intensity values with energies between 36 and 106 MeV/nuc. Also in the fit was the highest energy O data point at 94 - 125 MeV/nuc, scaled in intensity by the factor 1.095 to represent C. The resulting V1 GCR C spectrum in units of $(\mathrm{m}^2\ \mathrm{s\ sr\ MeV/nuc})^{-1}$ was $j_{V1} = 6.51 \times 10^{-5}$ T, where T is energy in MeV/nuc. For V2, a similar fit was made, except a C data point with energies 20 - 36 MeV/nuc was added to the fit. The resulting V2 GCR C spectrum was $j_{V2} = 5.59 \times 10^{-5}$ T. The assumed GCR abundances of the other species, relative to C, are: 107, 35.6, 0.228, 0.913, and 0.132 for H, He, N, O, and Ne. For N, O, and Ne, these ratios are from Simpson (1983) and represent observed GCR ratios at 70 - 280 MeV/nuc at 1 AU. For He, we use the estimate from Simpson (1983) at 600 - 1000 MeV/nuc. For H, we estimate a ratio of GCR H/He = 3 from our observed V1 H and He energy spectra. This ratio is smaller than the value of 4.7 $\pm$ 0.5 derived by Simpson (1983).

The ACR He shock spectrum is assumed to be a power-law in energy per nucleon, $dJ/dT = j_{He} \cdot T^{\gamma}$. The shock spectra of the other elements are assumed to be a power-laws with the same index. For O this is an adequate approximation for energies up to $\sim$ 10 MeV/nuc and for ACR He this approximation is valid up to $\sim$ 60 MeV/nuc (see Stone et al. (1996) for more discussion). Above a total energy of $\sim$ 150 - 240 MeV the energy spectra of these elements exhibit an approximately exponential roll-off (Stone et al., 1996).

We assume the diffusion coefficient, κ (in $\mathrm{cm}^2\ \mathrm{s}^{-1}$), is given by

$$\kappa = \frac{\kappa_0 \beta r (1+\kappa_S^2) R^2}{1 + (\kappa_S R)^2} \qquad (r \gg 1\ \mathrm{AU}) \tag{2}$$

where κ_0 and κ_S are scaling factors, β is particle speed, *r* is heliocentric radial distance in AU, and R is rigidity in GV. This form was used by Stone et al. (1996) and can be derived from the quasilinear formulation of Bieber et al. (1995). There are ten free parameters in the model: the shock location (r_S), the diffusion coefficient scaling factor (κ_0), the diffusion coefficient shape factor (κ_S), the power-law index (γ) of the energy spectrum at the shock, the intensity scaling factor (j_{He}) of the ACR He shock spectrum, and the ratios of the intensity scaling factors of the other elements to that of ACR He at the shock (H/He, C/He, N/He, O/He, and Ne/He). We assume that the solar wind velocity, V, is 500 km s^{-1}, which is close to the average value at V2 of 490 km s^{-1} for 1993/1 - 1994/365 (Richardson, private communication, 1995). The fits are not sensitive to the actual value of V, but a different V would result in a proportionally different κ_0.

The data and best-fit model curves for the period 1994/157-313 are shown in Figures 2a-f. The fits were made only in the energy regions shown by the solid lines, below the exponential roll-off. The χ^2 of the ten-parameter best fit to the 86 data points participating in the fits in Figure 2 is 51.2. Figure 3 shows the best-fit diffusion coefficient as a function of rigidity.

We investigated the confidence limits for each parameter in two ways. We first estimated the 68% confidence limits by iteratively changing and fixing the value of one parameter and re-fitting until we found the parameter value where the χ^2 had increased by 1 (see Press et al. (1992)). We did this in turn for all ten parameters. The best-fit parameter values and the 68% confidence limits are shown in Table II for the period 1994/157-313.

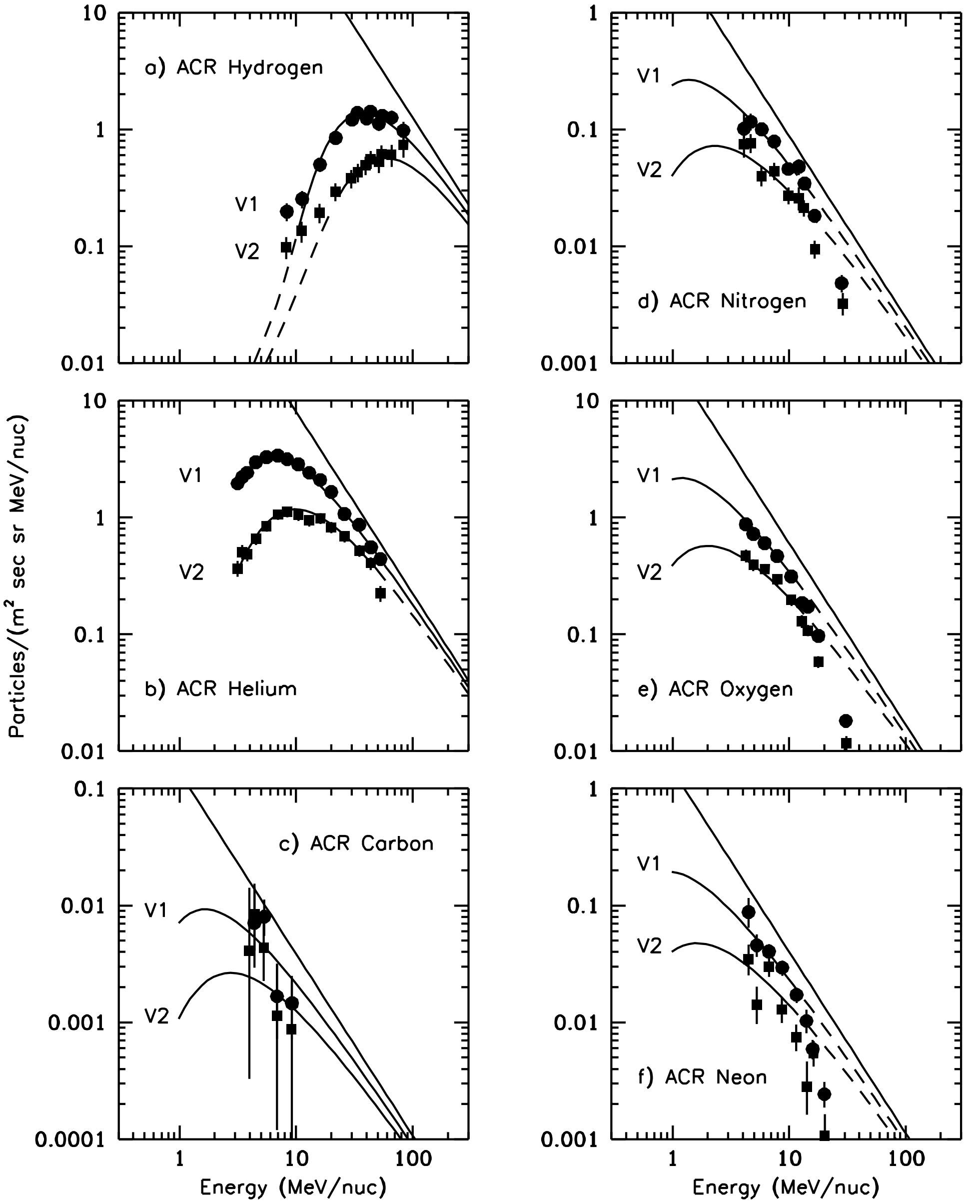

Figure 2. ACR energy spectra at the positions of V1 and V2 spacecraft for the period 1994/157-313. The curves represent the 10-parameter best-fit energy spectra at the solar wind termination shock, V1, and V2, as described in the text. a) ACR H, b) ACR He, c) ACR C, d) ACR N, e) ACR O, and f) ACR Ne.

In the second method we account for modelling uncertainties by using the estimated uncertainty in the effective radial position of V2 (0.5 AU). We performed two additional fits, one using the upper limit for the effective radial location for V2 and another using the lower limit. The resulting parameters are shown as the model limits in Table II.

For the shock distance, we need to apply an additional correction to account for the small but finite latitudinal gradient. In the study by Stone et al. (1996), the authors took

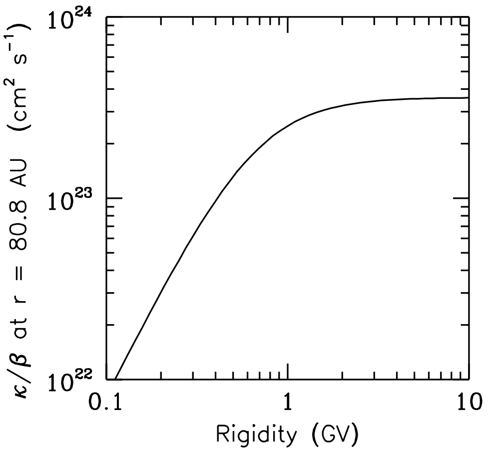

Figure 3. Best-fit diffusion coefficient divided by particle velocity versus rigidity at 80.8 AU. The form of the diffusion coefficient is described in the text.

Table II
Fit parameters for period 1994/157-313

Parameter*	Fit Value**	68% Lower Limit	68% Upper Limit	Model Lower Limit	Model Upper Limit
γ	-1.55 (-0.06, +0.03)	-1.62	-1.53	-1.56	-1.55
r_S (AU)	80.8 (-3.0, +2.4)***	77.9	82.9	81.7	79.8
κ_0 ($\times 10^{21}$)	3.10 (-0.22, +0.17)	2.92	3.22	3.23	2.98
κ_S	1.51 (-0.09, +0.11)	1.42	1.62	1.49	1.54
j_{He}	285 (-69, +81)	217	366	288	279
H/He	5.6 (-0.5, +0.6)	5.1	6.2	5.7	5.5
C/He ($\times 10^{-4}$)	4.8 ($\pm$ 1.1)	3.7	6.0	4.8	4.9
N/He ($\times 10^{-2}$)	1.1 ($\pm$ 0.1)	1.0	1.2	1.1	1.1
O/He ($\times 10^{-2}$)	7.5 ($\pm$ 0.6)	7.0	8.1	7.5	7.7
Ne/He ($\times 10^{-3}$)	5.0 ($\pm$ 0.4)	4.6	5.5	5.0	5.1

* See text for definition of symbols.
** Approximate uncertainty in parenthesis derived from the root mean square of the statistical (68%) uncertainty and the model uncertainty. The model uncertainty illustrates the change in the best-fit values resulting from an uncertainty of $\pm$ 0.5 AU in the effective radial location of V2.
*** Shock location estimate taking account of finite latitudinal gradient is 100 $\pm$ 6 AU (see text).

account of this effect by making a correction to the radial locations of V1 and V2 before using the spherically-symmetric model to fit the energy spectra. The correction they derived was

$$\ln(r'/r_{act}) = (G_\Theta \cdot \Theta / G_0) \tag{3}$$

where r' is the effective location, r_{act} is the actual location, G_Θ is the average latitudinal gradient, and Θ is the absolute value of the latitude of the spacecraft, and where a model was used in which the radial gradient in the intensity j is proportional to $1/r$, with

$(1/j)(\partial j/\partial r) = G_0/r$. In the current study, we make a correction to the radial location of V2 to account for the transient intensity decrease observed on V2. The fits are then made with the actual V1 radial location and the transient-decrease-corrected radial location of V2. Thus the resulting shock location, r_S, is a first-order estimate of the location if there were no latitudinal gradient. To derive a correction factor to apply to r_S, we assume that the ratio of intensities at two locations can be described by the following equation:

$$j_0 = j_1 \exp[-\int_{r_0}^{r_1} (CV/\kappa)dr] \tag{4}$$

where j_i is the intensity at radial location r_i, C is the Compton-Getting factor, V is the solar-wind speed, and κ is the diffusion coefficient. We assume that the diffusion coefficient is proportional to radial distance, $\kappa = \kappa_1 \cdot r$, so that Equation 4 can be written

$$\ln(j_0/j_1) = -(CV/\kappa_1)\ln(r_1/r_0) \tag{5}$$

where r_1 and r_0 are the radial locations where the intensities j_1 and j_0 are measured, respectively. Thus,

$$\frac{\ln(j_0/j_1)}{\ln(r_1/r_0)} = \text{constant} \tag{6}$$

By applying Equation 6 for two cases: 1) $r_1 = r_S$ and $r_0 = r_{V1}$ and 2) $r_1 = r_{V1}$ and $r_0 = r_{V2}$ we find

$$\frac{\ln(r_S/r_{V1})}{\ln(r_{V1}/r_{V2})} = \frac{\ln(j_{V1}/j_S)}{\ln(j_{V2}/j_{V1})} \tag{7}$$

If we substitute the latitude-corrected spacecraft positions for the actual positions, the best-fit shock position should change such that the same shock flux j_S and the fluxes j_{V1} and j_{V2} are recovered. Since the right side of Equation 7 will remain unchanged, so must the left side. That is,

$$\frac{\ln(r_S^{'}/r_{V1}^{'})}{\ln(r_{V1}^{'}/r_{V2}^{'})} = \frac{\ln(j_{V1}/j_S)}{\ln(j_{V2}/j_{V1})} \tag{8}$$

and thus

$$\ln({r_S}'/{r_{V1}}') = \ln(r_S/r_{V1})\frac{\ln({r_{V1}}'/{r_{V2}}')}{\ln(r_{V1}/r_{V2})} \tag{9}$$

From Equation 3,

$$\ln({r_{V1}}'/r_{V1}) = (G_\Theta \cdot \Theta_{V1}/G_0) \tag{10}$$

and

$$\ln({r_{V2}}'/r_{V2}) = (G_\Theta \cdot \Theta_{V2}/G_0) \tag{11}$$

By using these two equations in Equation 9, it can be shown that

$$\ln({r_S}'/{r_{V1}}') = a\ln(r_S/r_{V1}) \tag{12}$$

where

$$a = 1 + \frac{G_\Theta}{G_0} \frac{(\Theta_{V1} - \Theta_{V2})}{\ln(r_{V1}/r_{V2})} \tag{13}$$

Using Equations 10, 12, and 13, it can be shown that

$$\frac{{r_S}'}{r_S} = (\frac{r_S}{r_{V1}})^b \exp(G_\Theta \cdot \Theta_{V1}/G_0) \tag{14}$$

where $b = a - 1$. Using the values of $G_\Theta = 0.78 \pm 0.18$ %/deg, and $G_0 = 1.96 \pm 0.19$ from Stone et al. (1996), and $r_S = 80.8$ AU from Table II, we find ${r_S}'/r_S = 1.24 \pm 0.07$. Applying this correction to the derived fit shock location from Table II, we find ${r_S}' = 100{\pm}6$ AU. We caution, however, that this estimate is based on Equation 5 which is only an approximation to the solution of the full transport equation. No systematic error to account for this source of uncertainty has been added.

The shock strength (see, e.g., Potgieter and Moraal (1988)), s, is related to the spectral index by: $s = (2\gamma - 2)/(2\gamma + 1)$. From the values of γ in Table II, the inferred strength of the shock is 2.42 (-0.08, +0.04). The shock is not a strong shock (s = 4; γ = -1), a finding in agreement with the results from the study by Stone et al. (1996).

3. Injection Efficiency of Pickup Ions at Shock

To estimate the efficiency ϵ_i for the injection of pickup ion species i into the acceleration process, we follow the calculations of Lee (1983) from which it can be shown that the accelerated spectrum is given in units of $(\mathrm{cm}^2\ \mathrm{s\ sr\ MeV/nuc})^{-1}$ by

$$j = p^2 f(p) = \frac{\nu \epsilon_i F_i}{4\pi}\ E_{0i}^{(\nu-4)/2}\ E^{(-\nu+2)/2} \tag{15}$$

where $\nu \equiv 3/(1 - \rho_u/\rho_d) = 5.11$ for a downstream/upstream density ratio of 2.42, $F_i(\mathrm{cm}^{-2}\ \mathrm{s}^{-1})$ is the pickup ion flux at the shock, and E_{0i} is the injection energy corresponding to $2V_{SW}$, taken here to be 5.2×10^{-3} MeV/nuc. The pickup ion fluxes at the shock can be estimated from the observations of Geiss et al. (1994), who inferred the densities of neutral H, He, C, N, O, and Ne in the outer heliosphere shown in Table III. Using these values, the model of Vasyliunas and Siscoe (1976) for the distribution of these neutrals throughout the heliosphere, and the long-term ionization rates at 1 AU from Rucinski et al. (1996) (also shown in Table III), we estimate the fluxes of H^+, He^+, O^+, and Ne^+ pickup ions at the nose of the heliosphere shown in Table III and displayed in Figure 4. We do not include the pickup ion fluxes of C^+ in Table III because the neutral density of C from the pickup ion studies is only an upper limit. The N^+ pickup ion flux is also missing from Table III because we could not find the charge-exchange cross section for N and hence we could not independently estimate the long-term ionization rate of N at 1 AU. Later, we will use our observations to make estimates of these parameters for N and of the neutral C density in the outer heliosphere.

Equation 15 can be written:

$$j_i = D_i\ \epsilon_i\ E^{-1.55}\ (\mathrm{m}^2\ \mathrm{s\ sr\ MeV/nuc})^{-1} \tag{16}$$

where the coefficients D_i are shown in Table IV. These are the calculated ACR spectra at the shock and they can be compared with the derived ACR shock spectra from the model

Table III
Pickup ion parameters

Element	Neutral abund. in outer heliosphere*	Total ioniz. rate at 1 AU** ($\times 10^{-7}$ s^{-1})	Pickup ion flux at nose of heliosphere (cm^{-2} s^{-1})
H	7.7 ± 1.3	7.44 ± 0.16	10240
He	1.00***	1.08 ± 0.10	228
C	$\leq 0.8 \times 10^{-3}$	10.35 ± 0.77	
N	0.5 (-0.3, +0.5) $\times 10^{-3}$		
O	3.5 (-1.4, +1.8) $\times 10^{-3}$	7.75 ± 0.41	5.3
Ne	0.7 (-0.5, +1.0) $\times 10^{-3}$	3.52 ± 0.33	0.53

* (Geiss and Witte, 1996; Gloeckler, 1996)
** (Rucinski et al., 1996)
*** Neutral density = 0.0155 ± 0.0025 cm^{-3} (Geiss and Witte, 1996)

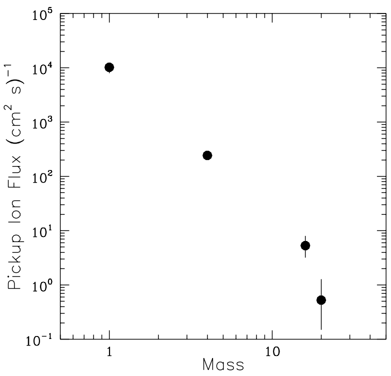

Figure 4. Estimated fluxes of pickup ions at the nose of the heliosphere at 100 AU, the estimated location of the solar wind termination shock.

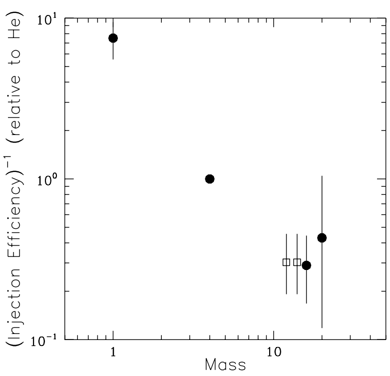

Figure 5. Estimated injection efficiencies of pickup ions into the acceleration process at the solar wind termination shock.

fits (Figure 2) to derive the relative injection efficiencies shown in Table IV. The relative efficiencies are much more reliably determined than the absolute efficiencies because the uncertainty in the spectral index is removed when the ratio is taken. The estimated uncertainties in the relative injection efficiencies include the uncertainties in the ACR intensity scaling factors from Table II and the uncertainties in the pickup ion fluxes, which are assumed to be dominated by the uncertainties in the neutral abundances from the pickup ion studies shown in Table III. It does not include any uncertainties associated with the simplifications inherent in the acceleration model in Equation 15. The relative injection efficiencies are shown as a function of particle mass in Figure 5. The observed preferential injection for the heavier particles is qualitatively consistent with Monte Carlo studies of shock acceleration by Ellison et al. (1981) but is in disagreement with the results of Kucharek and Scholer (1995).

Table IV
Injection efficiencies

Element	Coeff. D_i from Eq. 16	j_i from Table II	Inj. eff.	$(\text{Inj.eff.})^{-1}$ relative to He
H	2.25×10^6	1600	7.04×10^{-4}	7.5 (-2.5, +2.4)
He	5.34×10^4	285	5.29×10^{-3}	1.00
O	1.16×10^3	21.4	1.82×10^{-2}	0.29 (-0.12, +0.15)
Ne	1.16×10^2	1.43	1.23×10^{-2}	0.43 (-0.31, +0.62)

4. Ionization Rate of N at 1 AU

The open squares in Figure 5 represent weighted averages of the inverse injection efficiencies for O^+ and Ne^+. They are plotted at mass mumbers 12 and 14 to represent the estimated injection efficiencies of C^+ and N^+. For N^+, the value plotted, 0.30 (-0.11, +0.15) implies an absolute injection efficiency of 0.0174. From Table II we estimate that the ACR N shock spectral intensity coefficient is $j_N = 3.1$ which implies that the coefficient D_i for N (D_N) in Equation 16 is 3.1/0.0174 = 178. D_N is proportional to the flux of pickup ions at the shock. By scaling from the flux of He^+ pickup ions at the shock from Table III, we find that the expected flux of N^+ pickup ions at the shock is 0.81 cm^{-2} s^{-1}. Using the model of Vasyliunas and Siscoe (1976) for the distribution of neutrals in the heliosphere and the estimated neutral N density in the outer heliosphere from Table III (7.8 $\times$ 10^{-6} cm^{-3}), we estimate that the long-term ionization rate at 1 AU of neutral N must be $\sim$ 8.3 $\times$ 10^{-7} s^{-1}. This value is similar to that derived by Rucinski et al. (1996) for O (7.8 $\times$ 10^{-7} s^{-1}).

5. C Abundance

For C, only an upper limit to the neutral abundance in the outer heliosphere is available from the pickup ion observations. We can supply an estimate of this abundance by using a similar technique to that described above to deduce the ionization rate of N at 1 AU, except that in this case we have the long-term ionization rate of C from Table III and the unknown is the neutral abundance of C in the outer heliosphere. If we assume the injection efficiency for C^+ is as plotted in Figure 5, it can be shown that the neutral C density in the outer heliosphere must be 2.8 $(-1.0, +1.4)$ $\times$ 10^{-7} cm^{-3}, which implies the C/He ratio in the outer heliosphere is $1.8(-0.7, +0.9) \times 10^{-5}$. The uncertainty is estimated from the uncertainty computed for the injection efficiency for C^+ plotted in Figure 5 and the uncertainty in the neutral density of He in Table III. The neutral abundances of all the elements are shown in Figure 6. The abundances are plotted relative to He and for H, N, O, and Ne are from the pickup ion observations (Gloeckler, 1996; Geiss et al., 1994). For C, we show two abundances which are in good agreement, one from this study and one from Cummings and Stone (1990) derived from observations made during a solar minimum period in 1987.

6. Discussion

We consider the shock location derived from this study, 100 $\pm$ 6 AU, to be less accurate than the shock location of 85 $\pm$ 5 AU derived for a slightly different period (1994/157-209)

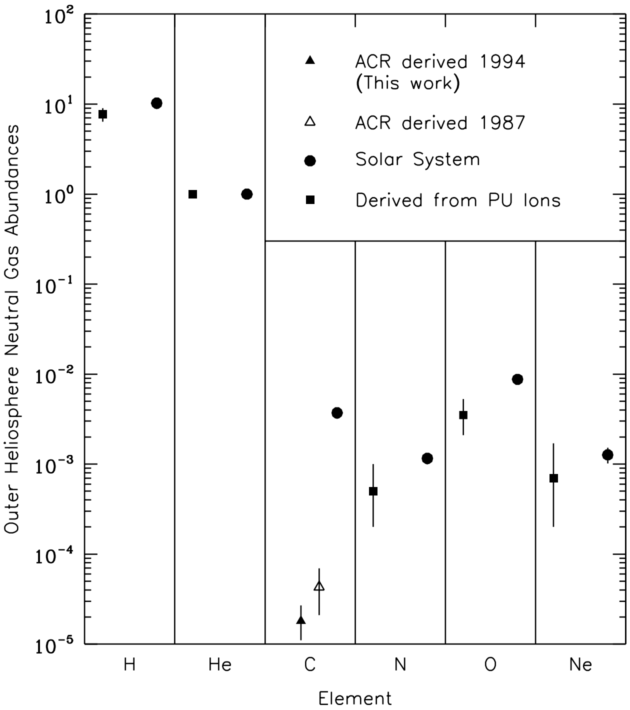

Figure 6. Estimated abundances of neutral gases in the outer heliosphere. The solid squares are from pickup ion studies (Geiss et al., 1996), the solid circles are solar system abundances (Grevesse and Anders, 1988), and the solid triangle is derived in this study.

by Stone et al. (1996). The reason is that the V1/V2 intensity gradients for the longer period considered in this study are typically larger than the average. Therefore, this period is likely affected by a transient or transients that have decreased the intensity at V2. While we have tried to take this into account by changing the location of V2 for the fits, the previous study has an advantage in that it used periods when there were apparently no transients present. We feel that the shock spectral intensity ratios are relatively insensitive to this effect and should be accurate. As evidence of this we find that the O/He ratios derived in the two studies are in good agreement. We also note that in Table II the model upper and lower limits for the intensity ratios and the spectral index are essentially the same as their respective nominal fit values.

The long-term ionization rate of neutral N derived in this study can be used to estimate the charge-exchange cross-section for the reaction $H^+ + N \rightarrow H + N^+$ for which we could find no reference in the literature. The study of ionization rates by Rucinski et al. (1996) did not address the charge-exchange process for N for that reason. However, that study did result in the estimate of 4.4×10^{-7} s^{-1} for the long-term photoionization rate of N at 1 AU. If we assume that the total ionization rate is due to photoionization and charge-exchange with the solar wind, then we estimate that the charge-exchange rate for N is $\sim 3.9 \times 10^{-7}$ s^{-1}. The long-term average solar wind flux is 3.9×10^{8} cm^{-2} s^{-1} (Rucinski et al., 1996), which implies that the cross-section for charge exchange is $\sim 1.0 \times 10^{-15}$ cm^{-2} at the average solar wind velocity of 450 km s^{-1} (1.1 keV).

The neutral C abundance derived in this study may be useful in estimating the ionization state of the very local interstellar medium (VLISM). Recently, Frisch (1995) used a previous estimate of the neutral C/O ratio = 0.0039 (-0.0020, +0.0039) from Cummings and Stone (1990), assuming the ratio in the outer heliosphere is the same as it is in the VLISM, to help deduce that the VLISM was likely highly ionized ($\sim$ 69 - 81%). From this study, we estimate that the neutral C/O ratio is 0.005 ± 0.003. The major reason for the change from the previous study is that the O in this study is from the pickup ion observations, whereas it was from the solar system abundances (Grevesse and Anders, 1988) in the previous study. We believe our current technique results in a more accurate estimate of the neutral C/O ratio. We caution, however, that our ratio represents an estimate for the outer heliosphere, just sunward of the termination shock, and filtering through the heliospheric interface has not been considered and may alter the ratio in the VLISM (see, e.g., Fahr et al. (1995)).

Acknowledgements

We are grateful to J. T. Hoeksema for providing the tilt observations prior to publication. We thank J. Richardson and J. Belcher for providing the Voyager 2 solar wind speed data. This work was supported by NASA under contract NAS7-918.

References

Bieber, J. W., Burger, R. A., and Matthaeus, W. H.: 1995, *Proc. Int. Conf. Cosmic Ray 24th*, **SH**, 694
Christian, E. R., Cummings, A. C., and Stone, E. C.: 1988, *Astrophys. J. Lett.*, **334**, L77
Christian, E. R., Cummings, A. C., and Stone, E. C.: 1995, *Astrophys. J. Lett.*, **446**, L105
Cummings, A. C., and Stone, E. C.: 1987, *Proc. Int. Conf. Cosmic Ray 20th*, **3**, 413
Cummings, A. C., and Stone, E. C.: 1988, Proc. Sixth Internat. Solar Wind Conference (Boulder), *NCAR Technical Note 306 2*, 599
Cummings, A. C., and Stone, E. C.: 1990, *Proc. Int. Conf. Cosmic Ray 21st*, **6**, 202
Ellison, D. C., Jones, F. C., and Eichler, D.: 1981, *J. Geophys.*, **50**, 110
Fahr, H. J., Osterbart, R., and Rucinski, D.: 1995, *Astron. Astrophys.*, **294**, 587
Fisk, L. A.: 1971, *J. Geophys. Res.*, **76**, 221
Fisk, L., Kozlovsky, B., and Ramaty, R.: 1974, *Astrophys. J. Lett.*, **190**, L35
Frisch, P. C.: 1995, *Space Sci. Rev.*, **72**, 499
Garcia-Munoz, M., Mason, G. M., and Simpson, J. A.: 1973, *Astrophys. J. Lett.*, **182**, L81
Geiss, J., Gloeckler, G., Mall, U., von Steiger, R., Galvin, A. B., and Ogilvie, K. W.: 1994, *Astron. Astrophys.*, **282**, 924
Geiss, J., and Witte, M.: 1996, *Space Sci. Rev.*, this issue
Gloeckler, G.: 1996, *Space Sci. Rev.*, this issue
Grevesse, N., and Anders, E.: 1988, *AIP Conference Proceedings*, **183**, 1
Hovestadt, D., Vollmer, O., Gloeckler, G., and Fan, C. Y.: 1973, *Phys. Rev. Lett.*, **31**, 650
Kucharek, H., and Scholer, M.: 1995, *J. Geophys. Res.*, **100**, 1745
Lee, M. A.: 1983, *J. Geophys. Res.*, **88**, 6109
McDonald, F. B., Teegarden, B. J., Trainor, J. H., and Webber, W. R.: 1974, *Astrophys. J. Lett.*, **187**, L105
McDonald, F. B., Lukasiak, A., and Webber, W. R.: 1995, *Astrophys. J. Lett.*, **446**, L101
Pesses, M. E., Jokipii, J. R., and Eichler, D.: 1981, *Astrophys. J. Lett.*, **246**, L85
Potgieter, M. S., and Moraal, H.: 1988, *Astrophys. J.*, **330**, 445
Press, W. H., Teukolsky, S. A., Vettering, W. T., and Flannery, B. P.: 1992, Numerical Recipes in C The Art of Scientific Computing, *Cambridge U. Press*, *2nd Ed.*, p551
Rucinski, D., Cummings, A. C., Gloeckler, G., Lazarus, A. J., Möbius, E., and Witte, M.: 1996, *Space Sci. Rev.*, this issue
Simpson, J. A.: 1983, *Ann. Rev. Nucl. Sci.*, **33**, 323
Stone, E. C.,Vogt, R. E., McDonald, F. B., Teegarden, B. J., Trainor, J. H., Jokipii, J. R., and Webber, W. R.: 1977, *Space Sci. Rev.*, **21**, 355
Stone, E. C., Cummings, A. C., and Webber, W. R.: 1996, *J. Geophys. Res.*, **101**, 11017
Vasyliunas, V. M., and Siscoe, G. L.: 1976, *J. Geophys. Res.*, **81**, 1247

Address for correspondence: A. C. Cummings, Mail Code 220–47, California Institute of Technology, Pasadena, CA 91125